

Photochemical & Photobiological Sciences

Accepted Manuscript



This is an *Accepted Manuscript*, which has been through the Royal Society of Chemistry peer review process and has been accepted for publication.

Accepted Manuscripts are published online shortly after acceptance, before technical editing, formatting and proof reading. Using this free service, authors can make their results available to the community, in citable form, before we publish the edited article. We will replace this *Accepted Manuscript* with the edited and formatted *Advance Article* as soon as it is available.

You can find more information about *Accepted Manuscripts* in the [Information for Authors](#).

Please note that technical editing may introduce minor changes to the text and/or graphics, which may alter content. The journal's standard [Terms & Conditions](#) and the [Ethical guidelines](#) still apply. In no event shall the Royal Society of Chemistry be held responsible for any errors or omissions in this *Accepted Manuscript* or any consequences arising from the use of any information it contains.



Photochemical & Photobiological Sciences

ARTICLE

Photosensitized degradation kinetics of trace halogenated contaminants in natural waters using membrane introduction mass spectrometry as an *in-situ* reaction monitor

Received 00th January 20xx,
Accepted 00th January 20xx

DOI: 10.1039/x0xx00000x

www.rsc.org/

Dane R. Letourneau,^{a,b} Chris G. Gill^{a,b} and Erik T. Krogh^{a,b}

The photochemically mediated dechlorination of polyhalogenated compounds represents a potential decontamination strategy and a relevant environmental process in chemically reducing media. We report the UV irradiation of natural and artificial waters containing natural dissolved organic matter to effect the photo-sensitized degradation of chlorinated organic compounds, including tetrachloromethane, 1,1,1-trichloroethane, perchloroethene, 1,2-dibromo-3-chloropropane and chlorobenzene at trace (ppb) levels in aqueous solution. The degradation kinetics are followed *in-situ* using membrane introduction mass spectrometry. By re-circulating the reaction mixture in a closed loop configuration over a semi-permeable hollow fiber polydimethylsiloxane membrane in a flow cell interface, volatile and semi-volatile compounds are continuously monitored using a quadrupole ion trap mass spectrometer. The time resolved quantitative information provides useful mechanistic insights, including kinetic data. Pseudo first-order rate constants for the degradation of contaminant mixtures in natural waters are reported.

1. Introduction

1.1. Halogenated contaminants

Environmental contamination by halogenated organic compounds remains a significant problem worldwide.^{1,2} Poor disposal strategies and inadequate and/or expensive remediation technologies have contributed to this problem. Over the last 25 years, environmental remediation efforts have consumed billions of dollars in the United States economy alone.^{3,4} The environmental impacts of halogenated compounds can be attributed in part to the strength of the carbon-chlorine bond and their hydrophobic character, leading to their increased persistence and tendency to bio-accumulate.² In addition to being recalcitrant, many halogenated organic compounds exhibit deleterious health effects and have the potential to bio-magnify in the food chain.⁴

A number of halogenated volatile organic compounds (VOCs) are of significant environmental concern due to their widespread use as industrial solvents or pesticides, their appearance in the environment (particularly in groundwater), and their associated toxicity. Table 1 outlines typical sources, groundwater concentrations, drinking water regulatory limits, hydrolysis half-lives, and toxicity information for five representative halogenated VOCs that are examined by this study.

1.2. Photodehalogenation

The electronegative character of halogenated substituents makes chlorinated organic compounds particularly good targets for transformations via reductive pathways.³ Polyhalogenated hydrocarbons are susceptible to reduction reactions in natural environments such as soils, sediments, and aquifers under anaerobic conditions.⁵ Reduction reactions typically remove at least one halogen, which in some cases can significantly reduce their persistence and toxicity.⁶ Examples of reductive strategies to remediate contaminated groundwaters include the introduction of passive reducing agents such as zero valent iron⁷ and active reducing systems such as electro-remediation.⁸ In addition, natural attenuation and reductive chemical transformations are known to be promoted by naturally occurring reducing agents, mediated by microbial processes and abiotic electron carriers.⁹ Photodehalogenation reactions can occur in the presence of photons of sufficient energy by either direct or indirect photolysis mechanisms. Direct photochemistry is limited to those compounds with a suitable chromophore. Indirect photolysis occurs via a light absorbing sensitizer, which then transfers energy to, or forms a reactive species for, the compound undergoing transformation. Photosensitized dehalogenation reactions are therefore not limited to contaminants with a chromophore, and can in principle be driven by solar radiation, provided the sensitizer absorbs at wavelengths greater than 300 nm.¹⁰

The degradation of a number of halogenated compounds (R-X) has been observed to occur via dissociative electron capture, where the initially formed radical anion loses a halide ion leaving a carbon centered radical.^{11,12} In the photohydrodehalogenation reaction, the halogen atom

^a Applied Environmental Research Laboratories, Department of Chemistry, 900 Fifth Street, Vancouver Island University, Nanaimo, BC V9R 5S5, Canada

^b University of Victoria, Department of Chemistry, PO Box 3065, Stn CSC, Victoria, BC, V8W 3V6, Canada.

(typically chlorine) is replaced by a hydrogen atom.¹³ Betterton et al has reported on this reaction as a potential treatment process for tetrachloromethane and several other halogenated compounds in aqueous solution.^{13,14} In this work, acetone was employed as the photosensitizer and 2-propanol as a sacrificial hydrogen donor (reductant). The reaction is thought to occur via hydrogen abstraction from 2-propanol by the excited triplet state (n, π^*) of acetone (similar to a Norrish type II mechanism¹⁵) followed by electron transfer to the alkyl halide and homolysis of the resulting radical anion. However, the absorption cross section of acetone requires the use of millimolar concentrations and high energy UV-C photons. Given that contaminated waters would need to be amended with relatively high concentrations of both acetone and 2-propanol, the applicability of this process for drinking water supplies is limited. Furthermore, the requirement for 254 nm photons is energy intensive and precludes the use of solar radiation. In the presented work, we explore the use of dissolved organic matter to photosensitize the dehalogenation reaction of trace contaminants in natural waters.

1.3. Natural organic matter and photo-sensitization

Natural organic matter (NOM) is a complex assemblage of biogenically derived organic compounds. Some fraction of this material is water soluble and referred to as dissolved organic matter (DOM). Humic and fulvic acids are classes of DOM operationally defined on the basis of the pH dependency of their water solubility. In addition to carboxylate and hydroxyl functional groups that impart water solubility, DOM molecules contain various chromophores including aromatic rings, conjugated ketones and alkenes. The specific UV absorbance (SUVA) is the dissolved organic carbon normalized absorbance and when measured at 254 nm is generally considered a surrogate measurement for the aromatic content of DOM.¹⁶⁻¹⁸ Because these chromophores absorb throughout the UV region tailing out to ~500 nm in the visible, waters with high DOM concentrations are often characterized by a distinct yellow/brown colour. The energy absorbed in this wavelength range can vary from 58–98 kJ mol⁻¹, making a number of indirect photochemical processes possible.¹⁰ Structural moieties within DOM have been observed to act as photosensitizers or precursors for the production of various reactive species in aquatic systems. These include hydroxyl radicals, singlet oxygen (¹O₂), solvated electrons (e⁻_(aq)), superoxide ion (O₂⁻), hydrogen peroxide and molecular hydrogen, all of which can be utilized to degrade a wide range of organic pollutants.^{10,19}

Photochemically derived, reactive DOM species can interact directly with other organic molecules via energy, electron or hydrogen atom transfer reactions,² typically via excited triplet states (³DOM*). Energy transfer reactions can induce cis/trans isomerizations,²⁰ while electron or hydrogen transfer reactions commonly lead to redox transformations of organic micropollutants.² Additionally, DOM has many redox-active functional groups, allowing it to serve as an electron shuttle.²¹ For example, quinone moieties play an important role in DOM-

mediated reductions.²² In particular, highly reactive hydrated electrons can play a significant role in the environmental photoreduction of persistent, electronegative pollutants²³, such as the halogenated contaminants investigated in this study. Figure 1 illustrates a scheme for the DOM-photosensitized degradation of a halogenated compound acting as an electron acceptor. In the presence of hydrogen atom donors, carbon-centered radicals abstract a hydrogen atom resulting in the corresponding R-H compounds.¹³

1.4. In-situ reaction monitoring with MIMS

Monitoring the progress of chemical reactions for trace organics traditionally involves discrete sampling at regular intervals, quenching steps (if required), and the subsequent sample work-up and analysis by conventional quantitative techniques (e.g., GC-MS). However, sample preparation and chromatographic separations can be time consuming, leading to limited kinetic information and loss of volatile analytes. Additionally, photochemical transformations are often studied at higher concentrations and/or in pure solvent systems, neither of which are necessarily good predictors of micropollutant transformations in natural systems. Membrane introduction mass spectrometry (MIMS) is a direct sampling technique that can be employed as an on-line quantitative analysis method for trace level analytes in complex samples.²⁴⁻²⁶ A membrane in direct contact with the sample is permeable to a suite of molecules, which are subsequently transferred to a mass spectrometer for resolution based upon their mass to charge ratio (m/z) and by unique fragmentations (e.g., tandem mass spectrometry (MS/MS)). The membrane, typically constructed of hydrophobic polydimethylsiloxane (PDMS), serves to reject the bulk of the sample matrix while pre-concentrating VOC and SVOC analytes from the sample. The overall sensitivity of the technique depends on the steady-state flux of analyte across the membrane as well as the efficiency of the ionization and m/z resolution. At the membrane level, the steady-state flux is given by eqn (1), where A is the surface area of the membrane in contact with sample, D is the diffusivity of the permeant (analyte) in PDMS, K is the partition co-efficient for the permeant between aqueous sample and PDMS membrane (approx. K_{ow}), C_s is the concentration of permeant in the sample, and l is the membrane thickness.²⁷

$$F_{ss} \propto \frac{ADKC_s}{l} \quad (1)$$

In general, thinner membrane interfaces increase flux and decrease the analytical response time. Various mass analyzers can be employed, providing selected m/z measurements in milliseconds with analytical sensitivities in the picogram range (ppt-ppb in solution). MIMS has been employed for the analysis of volatile organic compounds in air, water, and complex heterogeneous samples.^{26,28} By continuously operating the mass analyzer, MIMS systems can be used to provide temporally resolved data for multiple analytes in dynamic chemical systems.

The analyte signal response time in MIMS is limited by the kinetics of mass transport through the membrane (typically

seconds to minutes). Consequently, an analyte's characteristic signal risetime (τ) is a function of its intrinsic properties such as diffusivity (D), which depends largely on size (*i.e.*, molar volume) in addition to extrinsic factors including the membrane thickness (l)²⁷ as given by eqn (2).

$$\tau \propto \frac{l^2}{D} \quad (2)$$

Current MIMS systems are well suited for following dynamic processes that take place on a time scale of $\sim 10^2$ - 10^5 seconds (minutes to hours). As such, MIMS has been employed as an *in-situ* reaction monitor to follow the progress of a number of environmentally and industrially relevant reactions (for example, disinfection by-products,²⁹ biological processes,³⁰ the degradation of chlorinated organics,³¹ photosynthesis research,³² photolysis products,³³ and oxidative degradation of trace gasoline components³⁴), providing kinetically useful information. However, relatively few studies have used MIMS for the measurement of specific rate constants.³⁵⁻³⁷ In this study, we report the use of MIMS to directly assess the photo-sensitized degradation rate constants of five halogenated organic micropollutants in natural waters containing DOM.

2. Experimental

2.1. Standard and sample preparation

Commercially available reagents were used without further purification. Tetrachloromethane (CHROMASOLV[®], for HPLC, $\geq 99.9\%$), 1,1,1-trichloroethane (A.C.S. reagent, 99+%), 1,2-dibromo-3-chloropropane (97%), and perchloroethene (CHROMASOLV[®], for HPLC, $\geq 99.9\%$) were obtained from Sigma-Aldrich (Oakville, Ont., Canada). Chlorobenzene ($>95\%$) was supplied from Matheson Coleman & Bell (Gardena, CA, USA). Stock solutions (3000-5000 ppm) of halogenated contaminants were prepared gravimetrically in acetonitrile (Accusolv, HPLC grade, 99+%) using 40 mL clear glass sample vials equipped with Teflon[™] faced septa caps (EPA/VOA Type, Scientific Specialties Inc., Hanover, MD, USA). Aqueous standards were prepared in identical vials filled with high-purity deionized (DI) water (Model MQ Synthesis A10, Millipore Corp., Billerica, MA, USA) with little to no headspace. Volumetric injections (10-90 μ L) were delivered via gas tight syringes (VICI Precision Sampling Series C Syringes, Valco Instruments Co. Inc., Baton Rouge, LA, USA) through Teflon[™] faced septa into an in-house constructed 600 mL closed recirculation flask to yield final concentrations in the range of 0.1-20 ppb.

Calibration curves and characteristic signal risetimes were established for all five contaminant compounds using a series of stepwise injections of a combined standard into DI water in a temperature controlled re-circulation flask.

2.2. Natural water samples

Water from the Christina River (CR), a clear, brown coloured, nutrient rich surface water from Alberta, Canada that is typical of the northern boreal forest, was collected in June of 2010 and 2011 and stored in brown glass sample bottles at 25°C without

preservatives added. Water from Nanaimo River (NR), a clear, oligotrophic freshwater supply on Vancouver Island, British Columbia, Canada that is typical of a coastal surface water from the Pacific Northwest, was collected June of 2011 and stored in a similar fashion. All natural water samples were filtered with a 0.45 μ m membrane filter (Millipore Durapore, Billerica, MA, USA) prior to use. Artificial waters containing DOM were prepared from commercially available fulvic or humic acid isolates to provide reproducible waters for photosensitization experiments. A solution containing 10 mg/L of the sodium salt of humic acid (technical grade, Sigma-Aldrich, Oakville, ON, Canada) was dissolved in deionized water and used without further modification (henceforth referred to as AHA). A synthetic natural water was prepared according to the method of Izadifard et al³⁸ with 10 ppm Suwannee River fulvic acid (SRFA) (#1S101F, International Humic Substances Society, Denver, CO, USA), supplemented with 77 ppm calcium chloride ($\text{CaCl}_2 \cdot 2\text{H}_2\text{O}$, Anachemia) and 90 ppm sodium bicarbonate (Sigma-Aldrich, A.C.S. grade), with the pH of the solution adjusted between 7.1-7.3. Total organic carbon (TOC) measurements of all humic acid and natural water samples were performed with a Shimadzu TOC-V instrument (Columbia, MD, USA) as non-purgeable total organic carbon. Water quality parameters for natural and synthetic waters appear in Table 2 while the optical properties are displayed in Figure 2.

2.3. UV/vis and irradiance spectra

All UV/visible spectra of natural water samples and DOM amended solutions were collected with a UV/Vis spectrophotometer (Model 8453, Agilent, Mississauga, ON). Irradiance spectra for lamp and solar profiles were collected with a miniature UV/Vis spectrophotometer (Model EPP2000, StellarNet Tampa, Florida) equipped with a fibre-optic irradiance probe with a cosine diffuser (see Figure 2).

2.4. Experimental apparatus

A schematic diagram of the experimental apparatus is given in Figure 3. MIMS photolysis experiments were conducted in a closed 600 mL quartz vessel equipped with an internal cold finger and two side arm inlets positioned inside of a bench top photochemical reactor (Rayonet RPR-100, Southern New England Ultraviolet Company, Branford, CT) equipped with either eight 254 nm lamps (Model RPR-2540), sixteen 310 nm lamps (RPR-3000), or sixteen 370 nm lamps (RPR-3500) from the same supplier. The cold finger, recirculating 10°C water using a thermostat controlled water bath (Model 2095, Forma Scientific, Ottawa, ON, Canada), was used to control the temperature of the recirculating solution during photolysis.

Prior to adding halogenated contaminants, deionized water or other aqueous solution was re-circulated from the photochemical reservoir over the membrane interface through 0.25" O.D. Teflon[®] sample lines, while simultaneously sparging for 45 min with nitrogen (UHP Grade, 99.9999% Pure, Praxair, Nanaimo, BC, Canada) through a hypodermic needle with the system vented. Sample recirculation flow was maintained at 300 mL/min using a Masterflex L/S Easy-Load II peristaltic pump

(Model 77200-62, Cole-Parmer Ltd., Concord, Ont., Canada) equipped with Viton™ L/S 25 pump tubing. Sparging was ceased before beginning the MIMS experiment, and the baseline signal was stabilized for a minimum of 10 min on deionized water before injecting micropollutants.

2.5. Instrumentation

Experimental datasets were obtained using quadrupole ion-trap mass spectrometers: either a Polaris-Q system (Thermo-Fisher, San-Jose, CA, USA) or Saturn II system (Varian, Palo Alto, CA, USA) depending on availability. Each was equipped with a capillary hollow fiber polydimethylsiloxane (PDMS) membrane interface constructed in-house, with sample flowing over the outside of the membrane (10.0 cm length; I.D. 0.51 mm; O.D. 0.94 mm, Silastic brand®, Dow Corning, Midland, MI, USA).³⁴ The membrane was mounted in a flow-through cell constructed of 0.25" Swagelok™ (Supelco, Bellefonte, PA, USA) connectors and stainless steel tubing. Helium acceptor phase sweep gas (UHP grade, 99.999% pure, Praxair) flowing at ~1 mL/min through the lumen of the capillary hollow fiber membrane was used to transport volatile and semi-volatile permeating molecules to the quadrupole ion trap mass spectrometers (Polaris-Q system, 200°C ion source, Saturn II system, 80°C manifold temperature, both at a base pressure 1.0×10^{-5} Torr with heated transfer lines at 150°C). The Polaris-Q also employed a metal jet separator (Model MJSC/HP5890, 15 mL/min jets, SGE Corporation, Austin, TX, USA) backed at ~50 mTorr using a mechanical roughing pump (Edwards 5 E2M5, Edwards High Vacuum International, West Sussex, England). The membrane interfaces were mounted inside temperature programmable gas chromatograph ovens, which also served to regulate the He acceptor phase flows (Polaris-Q, 50°C via a Trace GC™, Thermo-Electron, San-Jose, CA, USA; Saturn II, 30°C via a Finnigan MAT GCQ Gas Chromatograph, Thermo-Fisher, San-Jose, CA, USA). Ionization for both systems was by EI (70 eV), the Polaris_Q utilizing an external ion source whereas the Saturn II employed internal ionization (directly within the ion storage volume of the trap).

Reaction progress was monitored by following five target analytes (individually and as a combined suite) using both full scan (m/z 50–250) and selected ion monitoring (SIM) modes. Isobaric interferences between the five contaminants were minimized using the SIM m/z reported in Table 3, which also gives intrinsic physico-chemical properties that influence membrane transport. For de-aerated solutions, molecular oxygen was monitored using SIM at m/z 32.

2.6. Actinometry and quantum yields

Chemical actinometry was used to measure the photon flux of the UV light sources used. An actinometer based on the photoreduction of aqueous tetrachloromethane to form chloroform in the presence of an acetone sensitizer and 2-propanol reductant was employed, according to Li et al.¹⁴ TCM and CHCl_3 were measured offline by gas chromatography (Finnigan Polaris-Q GC/MS system; Restek RTX-SMS Integra-Guard column 30 m X 0.25 mm X 0.25 μm ; isothermal 60°C;

100°C injector; He carrier, column head pressure 151.4 kPa; injection volume 1.0 μL). Under these conditions, tetrachloromethane disappearance and chloroform formation followed zero-order kinetics, where the slope of the linear decay curve was proportional to the number of photons absorbed for this well-characterized system. The 8 x 254 nm lamp set had a measured light flux of $3.4 \pm 1 \times 10^{-7}$ mol photons/min, and the 16 x 310 nm had a measured flux of $2.1 \pm 1 \times 10^{-7}$ mol photons/min. The photon flux was subsequently used to assess the quantum yield for loss of TCM in a natural water followed by MIMS and reported in Table 4.

2.7. MIMS data analysis

Detection limits for the five contaminants investigated here were estimated as three times the signal to noise ratio ($S/N = 3$) for a low concentration standard solution using the selected ion monitoring signals given in Table 3, chosen to minimize isobaric interferences observed for combined standard experiments (Table 3). The characteristic risetime of each compound was determined by analyzing the signal response for a step-function increase in analyte concentration in aqueous (DI) samples.³⁹ The normalized, time resolved MIMS signals were boxcar smoothed ($n=10$) and fitted to single exponential functions in the form of $S = 1 - e^{-kt}$ to obtain the characteristic risetime, $\tau = 1/k$. Since reaction dynamics occurring faster than membrane transport kinetics cannot be resolved by MIMS, we used the characteristic signal risetimes for each analyte to place an upper limit on the time constant for processes that can be followed by this approach, referred to herein as the 'kinetic limit'. It should be noted that the photo-degradation processes studied here are considerably slower than the upper limits imposed by membrane transport kinetics. Degradation decay curves were well described by single exponential fits. The slope of the log transformed data was used to obtain the observed first order degradation rate constants. The variance in the observed rate constants is independent of the MS instrument employed.

3. Results and discussion

3.1. MIMS Reaction Monitoring Characteristics

MIMS was characterized as an *in-situ* reaction monitor to follow the loss of several halogenated compounds during the photodegradation experiments in dilute aqueous solution. The estimated detection and kinetic limits for five halogenated compounds are reported in Table 3. Detection limits were typically observed in the 0.2-0.3 ppb range (nM), which is well below the US EPA drinking water guidelines for these compounds (Table 1). The sensitivity for 1,2-dibromo-3-chloropropane (DBCP) was diminished slightly by removing m/z 77 from the SIM due to an isobaric interference with CB. When DBCP is measured in the absence of chlorobenzene (CB), its detection limit is similar to the others. The characteristic risetimes under the conditions employed here range from 1 min for TCE to 3 min for DBCP and are correlated with molar volume. The kinetic limit is the inverse of the characteristic signal risetime and represents an upper limit for a first order reaction

rate constant that can be distinguished from membrane transport kinetics.³⁹ The characteristic risetimes and kinetic limits summarized in Table 3 are about an order of magnitude faster than the observed reaction kinetics (Table 5). Extrinsic factors that influence the magnitude of the kinetic limit include both temperature and membrane thickness. Higher temperatures and thinner membranes could be employed to study faster reaction rates, but were deemed unnecessary for the reactions investigated here.

3.2. Photochemistry Characteristics

A series of control experiments were carried out with tetrachloromethane (TCM) to establish conditions under which the photo-sensitized reaction occurs. Figure 4a shows the normalized signal intensity for TCM as a function of time during an *in-situ* reaction monitoring experiment. At 20 min, 10 ppb of TCM was added to a de-aerated aqueous solution containing AHA at 3.3 ppm C. After 30 min in the dark, there is no appreciable loss in signal intensity. At 55 min, the solution is irradiated at 254 nm and TCM signal is observed to decay over the course of several hours. Figure 4b shows the log transformed signal for TCM, which exhibits excellent first order behaviour over 10-90% of the decay. Control experiments in the absence of UV or humic substances show no loss of TCM. Since TCM has no chromophore that absorbs in the UV range investigated here, the reaction only proceeds in the presence of a photo-sensitizer, such as dissolved organic matter (DOM). The observed first order rate constant for this reaction is $0.028 \pm 0.005 \text{ min}^{-1}$ ($n=5$) under these conditions. The reaction proceeds under reducing conditions in the absence of dissolved oxygen, which is a known triplet quencher of $^3\text{DOM}^*$ and powerful electron acceptor. Figure 5a shows the log transformed degradation decay profiles for photo-degradation of TCM in the presence (aerated) and absence of dissolved oxygen (de-aerated). The reaction proceeds quite slowly in aerated solution. We estimate an upper limit for the decay constant in the presence of O_2 to be 0.004 min^{-1} , at least five times slower than that observed in de-aerated solution. This reaction was also investigated at several wavelengths. Figure 5b shows the log transformed decay profiles for TCM in CR (17 ppm C) at 254, 310 and 370 nm irradiation. The reaction proceeds slowly at 370 nm with an upper limit for the decay constant of 0.002 min^{-1} and nearly 40 times faster at 254 nm ($k = 0.081 \text{ min}^{-1}$). This is due to the significantly greater absorption of DOM at lower wavelengths as can be seen in Figure 2 as well as the slightly higher photon flux of the 254 nm lamps. Quantum yield estimates for the photo-degradation of TCM in CR at 254 and 310 nm are roughly 3×10^{-3} (Table 4) indicating that these are relatively inefficient reactions with most of the photonic energy being dispersed in competitive, non-productive processes. Based on our observations of first order kinetics and the effective quenching of the reaction by known electron scavengers (*i.e.*, O_2), we propose a differential rate law for the NOM photo-sensitized degradation of TCM in eqn (3).

$$\text{Rate} = d[\text{TCM}]/dt = k [\text{TCM}][e^-] = k_{\text{obs}} [\text{TCM}] \quad (3)$$

Under the steady-state photolysis conditions employed here, the effective concentration of hydrated electrons will remain constant, resulting in pseudo first order kinetic behaviour. Hence k_{obs} depends on the photon flux and efficiency of the electron transfer process. Although product studies were beyond the scope of this investigation, we do not observe the appearance of hydrodechlorination products (*e.g.*, CHCl_3 from TCM) under the reaction conditions investigated. While dissociative electron capture is well established for halogenated organic compounds,¹¹ the lack of appearance of any small hydrophobic molecules in our MIMS full mass scans, even in the presence of added hydrogen atom donors (*i.e.*, isopropyl alcohol, data not shown), suggests that the resulting carbon centred radicals may be incorporated into the complex DOM structures.

3.3. Photodegradation Kinetics of Different Compounds

The five halogenated contaminants included in this study were photolyzed at 254 nm, both individually and as a combined suite in de-aerated aqueous solutions. First order degradation rate constants were obtained *in-situ* using time resolved MIMS in deionized water and several natural waters containing DOM (Table 5). Neither TCM nor TCE showed any photochemical loss in the absence of DOM as a photosensitizer, due to the lack of chromophore for direct photolysis. We report a lower limit of 0.002 min^{-1} on the rate constant for these compounds to account for any minor signal drift over the long monitoring times ($> 4 \text{ hrs}$) required. In contrast, PCE, DBCP and CB were observed to undergo direct photolysis with first order rate constants of 0.30, 0.041 and 0.11 min^{-1} , respectively. Thus, the order of reactivity for equimolar (65 nM) de-aerated aqueous solutions without photosensitizer is as follows with the relative rates given in brackets:

$$\text{PCE} (>150) > \text{CB} (>55) > \text{DBCP} (>21) \gg \text{TCE} \sim \text{TCM} (1)$$

The photo-degradation of TCM and TCE was significantly enhanced (increasing by over an order of magnitude) in natural waters, where the reaction is photo-sensitized by DOM (Table 5). The degradation of contaminants such as PCE and CB that are capable of undergoing direct photolysis at 254 nm is actually inhibited in the presence of DOM (Table 6), as competition for photons reduces the steady-state population of excited PCE and CB. In Suwanee river fulvic acid (SRFA), TCM and PCE are observed to decay with the same apparent first order rate constant of 0.16 min^{-1} , followed by CB, DBCP and TCE. The relative rate for the reductive photo-degradation for these compounds in SRFA is given by:

$$\text{TCM} \sim \text{PCE} (5.3) > \text{CB} (2.0) > \text{DBCP} (1.9) > \text{TCE} (1)$$

MIMS offers the ability to simultaneously monitor the decay of multiple analytes, at different m/z values, in the same sample solution. This is demonstrated in Figure 6, where the loss of five compounds (65 nM) is followed in a natural river water sample

(CR). This capability provides us with the opportunity to investigate any synergistic and/or competitive effects, and is more representative of an environmentally relevant or industrial process water sample, where contamination by individual compounds is unlikely. In general, the measured rate constants obtained from individual runs are similar to those obtained in combined suites. For example, the rate constant for TCM in de-aerated water containing AHA (3.3 ppm C) was observed to be 0.028 and 0.027 min^{-1} when measured individually and in a combined suite, respectively (Table 5). With the exception of DBCP, which experienced a slight loss in sensitivity when corrected for isobaric interference with CB, the observed first-order decay constants for the other halogenated compounds are also in good agreement. In addition to providing greater environmental relevance, being able to monitor the simultaneous decay kinetics of multiple contaminants has a significant time saving advantage: Photolysis of the combined suite of compounds in CR water was completed in a few hours, yielding five first order rate constants. The relative rate for the reductive photo-degradation in CR water is given by:

$$\text{TCM} \sim \text{PCE} (4.4) > \text{DBCP} \sim \text{TCE} (1.6) > \text{CB} (1)$$

3.4. Photodegradation Kinetics in Different Natural Waters

Reductive photo-degradation reactions of representative halogenated organic compounds were directly followed in de-aerated aqueous solutions containing natural organic matter. The dissolved organic carbon concentrations in these solutions ranged from 1.4 ppm C (NR) to 18 ppm C (CR) as summarized in Table 2. The absorption spectra of natural waters appear in Figure 2 illustrates that CR has the greatest absorption extending out to ~ 500 nm, followed by the solution containing AHA (3.3 ppm C). Solutions of SRFA (5.3 ppm C) and NR were colourless, although they had significant absorbance at 254 nm. It is important to note that the different origin of the NOM in these samples will result in different compositional distribution of chromophores and hence photo-physical properties. This is illustrated by the carbon normalized SUVA_{254} values reported in Table 2. The higher SUVA_{254} values are consistent with a greater contribution of more strongly UV absorbing aromatic and conjugated moieties in the NOM.¹⁷ These values range from 2.2 for SRFA to 10. ($\text{ppm C}^{-1} \text{m}^{-1}$) for AHA and are presented in Table 2.

When the rate constants for the 254 nm photo-degradation of TCM in four DOM containing waters are compared (Table 5), it is clear that photolysis is fastest in water containing SRFA with an observed rate constant of 0.16 min^{-1} . Photolysis in CR proceeded at about half this rate (0.098 min^{-1}), followed by AHA with a rate constant of 0.028 min^{-1} and NR with k_{obs} of 0.015 min^{-1} . Because these waters differ widely in their concentration and composition of DOM as well as their optical properties, it is useful to correct the apparent rate constants for light screening and amount of carbon present as has been done by others.^{16, 40} The carbon normalized rate constants for TCM indicate that SRFA is still the most efficient at promoting photo-degradation with a rate constant of 0.030 $\text{min}^{-1} (\text{ppm C})^{-1}$. NR is the second

most efficient on a per carbon basis with a normalized rate constant of 0.011 $\text{min}^{-1} (\text{ppm C})^{-1}$. It has been previously noted that although isolated humic substances (e.g., AHA) do indeed produce low yields of hydrated electrons, their quantum yields are not representative of all natural waters.¹⁹ Indeed, humic substances may not be the principal e^- producing component of natural waters - other UV-B absorbing chromophores (i.e., indoles such as tryptophan, or aromatic carboxylic acids) may be more important.¹⁹ Since CR contains considerably more dissolved organic carbon, its carbon normalized rate constant is the lowest at 0.0054 $\text{min}^{-1} \text{ppm C}^{-1}$, likely a result of light screening effects (*vide infra*). Thus, both the apparent and the carbon normalized decay rates of TCM are observed to vary over one order of magnitude between various DOM containing waters investigated, with SRFA appearing to be the most efficient in promoting the reaction. The SRFA may have a greater photosensitizing ability because it contains a greater fraction of the more highly water soluble hydroxylated aromatic carboxylic acids, which have been shown to be very effective electron donors under UV irradiation.^{37,41}

In general, the rate of reductive photo-sensitized degradation is expected to be controlled by the concentration of hydrated electrons in solution, which in turn will be governed by the composition and concentration of DOM, as well as the flux of energetic photons.¹⁹ Thus, depending on conditions, the kinetics of the reaction can be either photon or DOM limited. For example, at very high DOM concentrations, it is expected that the kinetics will be slower because light will not penetrate very far into an optically dense solution (light screening by DOM). Furthermore, since DOM can itself act as an electron scavenger,³⁴ the reaction will be photon limited. At the other extreme of very low DOM concentrations, the photo-sensitized reaction kinetics will be limited by the amount of DOM present. These effects can be observed in the first order rate constants for the degradation of the five micropollutants in a dilution series of CR ranging from 18 ppm C to 1.4 ppm C (Table 6). For PCE and CB, which have been shown to undergo direct photolysis under these conditions (*vide supra*), we observe a trend towards faster decay constants in progressively more dilute DOM solutions. This is consistent with a competition for photons between the contaminant and the DOM molecules. On the other hand, for TCM and TCE, which can only undergo photo-sensitized degradation, the rate of the first order decay goes through a maximum at intermediate DOM concentrations.

Investigating the effect of DOM concentration on the photo-sensitized dehalogenation reaction kinetics led to an unexpected result, which illustrates power of using sensitive and selective time resolved techniques such as MIMS as an *in-situ* reaction monitor. In some of the experiments following the decay of TCM, two distinct kinetic regimes were observed (Figure 7). During the initial phase of the photochemical reaction, the loss of TCM follows zeroth order kinetics. Using a SIM at m/z 32 to monitor for molecular oxygen, we observe a slow rise in the concentration of O_2 after de-aeration and before the UV lamps are turned on, indicating a slow leak of oxygen into our closed loop reaction system. Once the photochemistry is initiated, the oxygen concentration drops sharply as O_2

effectively scavenges electrons, converts to superoxide ion, and undergoes subsequent chemistry.³⁷ Only when the signal at m/z 32 drops to zero, and the O₂ has been completely scrubbed out of solution, do the TCM kinetics convert to first order behaviour. Thus, simultaneously monitoring different reactants and/or interferences using *in-situ* mass spectrometry techniques provides mechanistic insights that might easily be overlooked using conventional off-line analytical techniques.

4. Conclusion

Membrane introduction mass spectrometry has been employed as an on-line monitoring strategy to directly follow the photo-degradation kinetics of five representative volatile and semi-volatile halogenated organic compounds in dilute aqueous solution including complex natural waters. Detection limits were less than 1 µg/L (nM range), which is environmentally relevant, and below drinking water regulatory limits. Membrane permeation kinetics had observed time constants greater than 0.002 min⁻¹, imposing upper limits on the fastest measurable reaction rates (kinetic limits) possible with the described methodology. Faster reactions can be investigated with thinner membranes and/or higher membrane temperatures.

We observe first-order photo-degradation kinetics for the five representative halogenated organic micropollutants examined in de-aerated aqueous solutions, including natural waters, with quantum yields in the 10⁻³ range. We report first order rate constants ranging from 0.002 to 0.30 min⁻¹, and compare relative reaction rates in a variety of natural waters. Compounds without a chromophore (*i.e.*, TCM and TCE) are unreactive in the absence of a dissolved organic matter (DOM) but experience enhanced photo-sensitized degradation in de-aerated waters containing a photo sensitizer. Compounds that contain a chromophore (*i.e.*, PCE and CB) undergo direct photolysis, and waters containing high DOM inhibit the degradation kinetics by competing for photons.

We demonstrate the advantages of using MIMS as an *in-situ* reaction monitor to simultaneously follow the reaction dynamics of multiple compounds at nanomolar concentrations in complex natural samples. This provides a direct measure of reaction kinetics at environmentally relevant concentrations, and allows for direct comparison of degradation rates of various compounds under a variety of environmental conditions. While the unit mass resolution employed here may suffer isobaric interferences from unknown components in complex samples, tandem MS and/or the use of higher resolution mass analysers can, in principle, be employed to mitigate these challenges. Furthermore, the power of the technique in providing mechanistic insight is exemplified by the observation of different kinetic regimes (*e.g.*, zeroth order behaviour) in the decay kinetics of TCM in CR, triggered by the complete consumption of dissolved molecular oxygen.

Future studies including the use of specific photo-sensitizers (*e.g.*, model compounds), particularly those absorbing at longer wavelengths using solar irradiance are currently underway.

Acknowledgements

This project would not have been possible without the contributions of several AERL group members, particularly Janet Nelson, Tim MacInnis, and Cameron Newhook. The authors gratefully acknowledge Vancouver Island University and the University of Victoria for their on-going support of students in the Applied Environmental Research Laboratories. The authors are grateful for the financial support of this work provided by the Natural Science and Engineering Research Council (NSERC) of Canada through the Discovery (DG 298325) and USRA programs.

References

- 1 D. C. G. Muir and P. H. Howard, Are there other persistent organic pollutants? A challenge for environmental chemists, *Environ. Sci. Technol.*, 2006, 40, 7157-7166.
- 2 R. P. Schwarzenbach, P. M. Gschwend and D. M. Imboden, *Environmental Organic Chemistry*, Wiley, 2003.
- 3 J. H. He, W. P. Ela, E. A. Betterton, R. G. Arnold and A. E. Saez, Reductive dehalogenation of aqueous-phase chlorinated hydrocarbons in an electrochemical reactor, *Ind. Eng. Chem. Res.*, 2004, 43, 7965-7974.
- 4 P. K. Freeman and C. M. Haugen, Differential photohydrodehalogenation reactivity of bromobenzenes (1,2,4-tribromobenzene, 1,2,3,5-tetrabromobenzene) and pentachlorobenzene: Sunlight-based remediation, *J. Chem. Technol. Biotechnol.*, 1998, 72, 45-49.
- 5 G. P. Curtis and M. Reinhard, Reductive dehalogenation of hexachloroethane, carbon tetrachloride, and bromoform by anthrahydroquinone disulfonate and humic acid, *Environ. Sci. Technol.*, 1994, 28, 2393-2401.
- 6 J. Gan, Q. Wang, S. R. Yates, W. C. Koskinen and W. A. Jury, Dechlorination of chloroacetanilide herbicides by thiosulfate salts, *PNAS*, 2002, 99, 5189-5194.
- 7 W. Zhang, L. Li, B. Z. Li, K. F. Lin, S. G. Lu, R. B. Fu, J. Zhu and X. H. Cui, Mechanism and pathway of tetrachloroethylene dechlorination by zero-valent iron with Cu or Cu/C, *J. Environ. Eng.*, 2013, 139, 803-809.
- 8 X. Lu and S. Yuan, Electrokinetic removal of chlorinated organic compounds, in *Electrochemical Remediation Technologies for Polluted Soils, Sediments and Groundwater*, John Wiley & Sons, Inc., 2009, pp. 219-234.
- 9 J. A. Perlinger, J. Buschmann, W. Angst and R. P. Schwarzenbach, Iron porphyrin and mercaptojuglone mediated reduction of polyhalogenated methanes and ethanes in homogeneous aqueous solution, *Environ. Sci. Technol.*, 1998, 32, 2431-2437.
- 10 J. P. Aguer, C. Richard and F. Andreux, Effect of light on humic substances: Production of reactive species, *Analisis*, 1999, 27, 387-390.
- 11 M. Lal, C. Schoneich, J. Monig and K. D. Asmus, Rate constants for the reactions of halogenated organic radicals, *Int. J. Radiat. Biol.*, 1988, 54, 773-785.
- 12 A. Matsunaga and A. Yasuhara, Dechlorination of PCBs by electrochemical reduction with aromatic radical anion as mediator, *Chemosphere*, 2005, 58, 897-904.
- 13 E. A. Betterton, N. Hollan, R. G. Arnold, S. Gogosha, K. McKim and Z. J. Liu, Acetone-photosensitized reduction of carbon tetrachloride by 2-propanol in aqueous solution, *Environ. Sci. Technol.*, 2000, 34, 1229-1233.
- 14 H. Li, E. A. Betterton, R. G. Arnold, W. P. Ela, B. Barbaris and C. Grachane, Convenient new chemical actinometer based on aqueous acetone, 2-propanol, and carbon tetrachloride, *Environ. Sci. Technol.*, 2005, 39, 2262-2266.
- 15 N. J. Turro, V. Ramamurthy and J. C. Scaiano, *Principles of Molecular Photochemistry: An Introduction*, University Science Books, 2009.
- 16 Y. P. Chin, P. L. Miller, L. Zeng, K. Cawley and L. Weavers, Photosensitized degradation of bisphenol A by dissolved organic matter, *Environ. Sci. Technol.*, 2004, 38, 5888-5894.
- 17 E. C. Minor, M. M. Swenson, B. M. Mattson and A. R. Oyler, Structural characterization of dissolved organic matter: A review of current techniques for isolation and analysis, *Environ. Sci. Processes Impacts*, 2014, 16, 2064-2079.
- 18 J. L. Weishaar, G. R. Aiken, B. A. Bergamaschi, M. S. Fram, R. Fujii and K. Mopper, Evaluation of specific ultraviolet absorbance as an indicator of the chemical composition and reactivity of dissolved organic carbon, *Environ. Sci. Technol.*, 2003, 37, 4702-4708.
- 19 T. E. Thomas-Smith and N. V. Blough, Photoproduction of hydrated electron from constituents of natural waters, *Environ. Sci. Technol.*, 2001, 35, 2721-2726.
- 20 R. G. Zepp, P. F. Schlotzhauer and R. M. Sink, Photosensitized transformations involving electronic-energy transfer in natural waters: Role of humic substances, *Environ. Sci. Technol.*, 1985, 19, 74-81.
- 21 S. H. Kang and W. Choi, Oxidative degradation of organic compounds using zero-valent iron in the presence of natural organic matter serving as an electron shuttle, *Environ. Sci. Technol.*, 2008, 43, 878-883.
- 22 F. M. Dunnivant, R. P. Schwarzenbach and D. L. Macalady, Reduction of substituted nitrobenzenes in aqueous solutions containing natural organic matter, *Environ. Sci. Technol.*, 1992, 26, 2133-2141.
- 23 R. G. Zepp, A. M. Braun, J. Hoigne and J. A. Leenheer, Photoproduction of hydrated electrons from natural organic solutes in aquatic environments, *Environ. Sci. Technol.*, 1987, 21, 485-490.
- 24 R. A. Ketola, T. Kotiaho, M. E. Cisper and T. M. Allen, Environmental applications of membrane introduction mass spectrometry, *J. Mass Spectrom.*, 2002, 37, 457-476.
- 25 R. C. Johnson, R. G. Cooks, T. M. Allen, M. E. Cisper and P. H. Hemberger, Membrane introduction mass spectrometry: Trends and applications, *Mass Spectrom. Rev.*, 2000, 19, 1-37.
- 26 N. G. Davey, E. T. Krogh and C. G. Gill, Membrane-introduction mass spectrometry (MIMS), *Trends Anal. Chem.*, 2011, 30, 1477-1485.
- 27 M. A. LaPack, J. C. Tou and C. G. Enke, Membrane mass spectrometry for the direct trace analysis of volatile organic compounds in air and water, *Anal. Chem.*, 1990, 62, 1265-1271.
- 28 E. T. Krogh and C. G. Gill, Membrane introduction mass spectrometry (MIMS): A versatile tool for direct, real-time chemical measurements, *J. Mass Spectrom.*, 2014, 49, 1205-1213.
- 29 J. T. Borges, R. Sparrapan, J. R. Guimaraes, M. N. Eberlin and R. Augusti, Chloroform formation by chlorination of aqueous algae suspensions: Online monitoring via membrane introduction mass spectrometry, *J. Braz. Chem. Soc.*, 2008, 19, 950-955.
- 30 F. R. Lauritsen and S. Gylling, Online monitoring of biological reactions at low parts-per-trillion levels by membrane inlet mass spectrometry, *Anal. Chem.*, 1995, 67, 1418-1420.
- 31 R. M. Alberici, M. A. Mendes, W. F. Jardim and M. N. Eberlin, Mass spectrometry on-line monitoring and MS2 product characterization of TiO₂/UV photocatalytic degradation of chlorinated volatile organic compounds, *J. Am. Soc. Mass. Spectrom.*, 1998, 9, 1321-1327.
- 32 K. Beckmann, J. Messinger, M. R. Badger, T. Wydrzynski and W. Hillier, On-line mass spectrometry: Membrane inlet sampling, *Photosynth. Res.*, 2009, 102, 511-522.
- 33 P. S. H. Wong, N. Srinivasan, N. Kasthurikrishnan, R. G. Cooks, J. A. Pincock and J. S. Grossert, On-line monitoring of the photolysis of benzyl acetate and 3,5-dimethoxybenzyl acetate by membrane introduction mass spectrometry, *J. Org. Chem.*, 1996, 61, 6627-6632.
- 34 J. H. L. Nelson, D. A. Friesen, C. G. Gill and E. T. Krogh, On-line measurement of oxidative degradation kinetics for trace gasoline contaminants in aqueous solutions and natural water by membrane introduction tandem mass spectrometry, *J. Environ. Sci. Health., Part A*, 2010, 45, 1720-1731.
- 35 R. Augusti, A. Dias, L. Rocha and R. Lago, Kinetics and mechanism of benzene derivative degradation with Fenton's

- reagent in aqueous medium studied by MIMS, *J. Phys. Chem. A*, 1998, 102, 10723-10727.
- 36 R. Rios, L. L. da Rocha, T. G. Vieira, R. M. Lago and R. Augusti, On-line monitoring by membrane introduction mass spectrometry of chlorination of organics in water: Mechanistic and kinetic aspects of chloroform formation, *J. Mass Spectrom.*, 2000, 35, 618-624.
- 37 F. Soltermann, S. Canonica and U. von Gunten, Trichloramine reactions with nitrogenous and carbonaceous compounds: Kinetics, products and chloroform formation, *Water Res.*, 2015, 71, 318-329.
- 38 M. Izadifard, personal communication, 2012.
- 39 D. W. Janes, C. J. Durning, D. M. van Pel, M. S. Lynch, C. G. Gill and E. T. Krogh, Modeling analyte permeation in cylindrical hollow fiber membrane introduction mass spectrometry, *J. Membr. Sci.*, 2008, 325, 81-91.
- 40 P. L. Miller and Y. P. Chin, Photoinduced degradation of carbaryl in a wetland surface water, *J. Agric. Food Chem.*, 2002, 50, 6758-6765.
- 41 R. M. Cory, J. B. Cotner and K. McNeill, Quantifying interactions between singlet oxygen and aquatic fulvic acids, *Environ. Sci. Technol.*, 2009, 43, 718-723.
- 42 U.S. Environmental Protection Agency, *Basic Information about Regulated Drinking Water Contaminants and Indicators*, 2015.
- 43 World Health Organization, *Guidelines for Drinking-water Quality, Fourth Edition*, Geneva, 2011.
- 44 U.S. Public Health Service: Agency for Toxic Substances and Disease Registry, *Toxicological Profile for Chlorobenzene*, Atlanta, GA, 1990.
- 45 J. H. Montgomery, *Groundwater Chemicals Desk Reference*, CRC Press, Boca Raton, 2007.
- 46 J. M. Michael, *Occurrence and Implications of Selected Chlorinated Solvents in Ground Water and Source Water in the United States and in Drinking Water in 12 Northeast and Mid-Atlantic States, 1993–2002*, U.S. Geological Survey, Reston, Virginia, 2005.

TABLES

Table 1 Contaminant sources and typical environmental concentrations

	Tetrachloromethane (TCM)	1,1,1-trichloroethane (TCE)	Perchloroethene (PCE)	1,2-dibromo-3-chloropropane (DBCP)	Chlorobenzene (CB)
Sources	Discharge from chemical plants and other industrial activities ⁴²	Discharge from metal degreasing sites and other factories ⁴²	Discharge from factories and dry cleaners ⁴²	Runoff/leaching from soil fumigant used on soybeans, cotton, pineapples, and orchards ⁴²	Discharge from chemical and agricultural chemical factories ⁴²
Typical Environmental Concentration Ranges ($\mu\text{g/L}$)	<5 in drinking water ⁴³	<20 in surface and groundwaters ⁴³	<3 in drinking water ⁴³	Up to a few $\mu\text{g/L}$ in drinking water ⁴³	<3 in waste effluent ⁴⁴
U.S. EPA Drinking Water Maximum Conc. Limit ($\mu\text{g/L}$)	5 ⁴²	200 ⁴²	5 ⁴²	0.2 ⁴²	100 ⁴²
Typical hydrolysis $t_{1/2}$ values (days)	14,600 at 25 °C ⁴⁵	343 ⁴⁶	264 at 25 °C ⁴⁵	13,870 at 25 °C ⁴⁵	Not hydrolyzed in the aquatic environment
Oral LD ₅₀ rat (mg/kg)	2800 ⁴⁵	10,300 ⁴⁵	3005 ⁴⁵	170 ⁴⁵	2910 ⁴⁵



Photochemical & Photobiological Sciences

ARTICLE

Photochemical & Photobiological Sciences Accepted Manuscript

Table 2 Water quality data for natural and synthetic waters used in photosensitization studies

Water sample	[DOC] ^a (ppm C)	pH	Sp. Cond. ($\mu\text{S cm}^{-1}$)	SUVA ₂₅₄ (ppm C ⁻¹ m ⁻¹)
Nanaimo River (NR) (June, 2011)	1.4	6.0	30	4.0
Christina River (CR) (June, 2010)	18	7.9	92	4.3
Aldrich Humic Acid (AHA)	3.3	5.8	4.3	10.
Suwanee River Fulvic Acid (SRFA)	5.3	7.2	210	2.2

^a measured as non-purgeable organic carbon

Table 3 Intrinsic and measured properties of substrates studied for MIMS experiments

	TCM	TCE	PCE	DBCP	CB
SIM (<i>m/z</i>)	117,119,121	97,99	164,166,168	155,157	112,114
Ion	CCl ₃ ⁺	CH ₃ CCl ₂ ⁺	CCl ₂ CCl ₂ ⁺	C ₃ H ₅ BrCl ⁺	C ₆ H ₅ Cl ⁺
Log K _{ow} ^a	2.77	2.49	2.88	2.96	2.78
Molar Volume (cm ³ /mol) ^a	96.73	99.55	102.2	112.9	101.4
Detection Limit ^b (ppb)	0.2	0.3	0.2	1	0.2
Signal Risettime (min)	1.3	1.0	2.2	3.0	2.3
Kinetic Limit (x10 ⁻² min ⁻¹)	77	97	45	33	43

^a Schwarzenbach et al.²

^b S/N = 3

Table 4 Initial quantum yields for tetrachloromethane loss in Christina River water

UV lamps	Mols CCl ₄ / min	Mol photons absorbed / min	Initial quantum yield
254 nm (x8)	9.09x10 ⁻¹⁰	3.4x10 ⁻⁷	2.7±0.2 x 10 ⁻³
310 nm (x16)	5.48x10 ⁻¹⁰	2.1x10 ⁻⁷	2.6±1 x 10 ⁻³

Table 5 First order rate constants for the decay of 65 nM contaminants under various conditions

	Observed rate constants (10^{-2} min^{-1})					Carbon Normalized (10^{-2} min^{-1} ppm C ⁻¹)
	TCM	TCE	PCE	DBCP	CB	TCM
8x254 nm						
DI water	<0.2	<0.2	30.	4.1	11.	<0.01
SRFA (individual)	16.	3.0	16.	5.6	5.9	3.0
NR (individual)	1.5	-	-	-	-	1.1
AHA (individual)	2.8±0.5 (n=5)	1.6	9.5	1.7	3.6	0.85
AHA (combined)	2.7	1.7	11.	3.4	4.4	0.82
CR (individual)	9.8±1.5 (n=4)	-	-	-	-	0.54
CR (combined)	7.0±0.5 (n=2)	2.4±0.5 (n=2)	6.8±2.2 (n=2)	2.7±1.2 (n=2)	1.6±0.7 (n=2)	0.39
16x310 nm						
CR (individual)	1.8	<0.2	<0.2	<0.2	<0.2	0.10
16x370 nm						
CR (individual)	<0.2	-	<0.2	-	<0.2	<0.01

Table 6 First order rate constants for the photo-degradation of 65 nM substrates in CR dilution series

[DOC] (ppm C)	Observed rate constants (10^{-2} min^{-1})				
	TCM	TCE	PCE	DBCP	CB
18	6.7	2.0	5.2	1.9	1.1
8.8	6.1	1.5	7.4	1.8	2.2
4.4	15	5.0	12	2.2	3.4
1.8	2.3	1.3	16	3.7	5.0
1.4	2.6	1.6	16	4.2	7.9

FIGURES

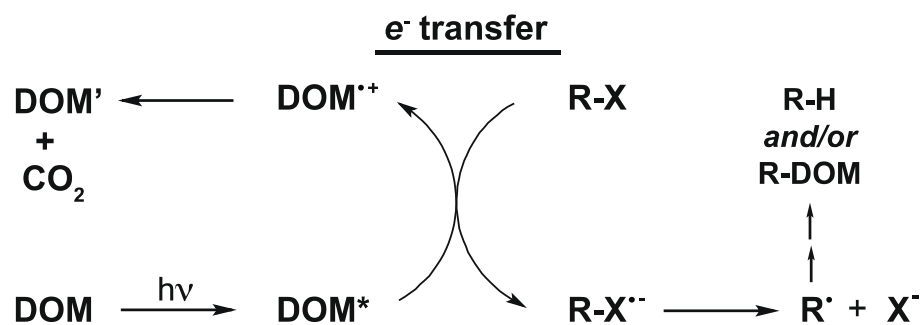


Fig. 1 DOM-mediation reductive photodehalogenation scheme.

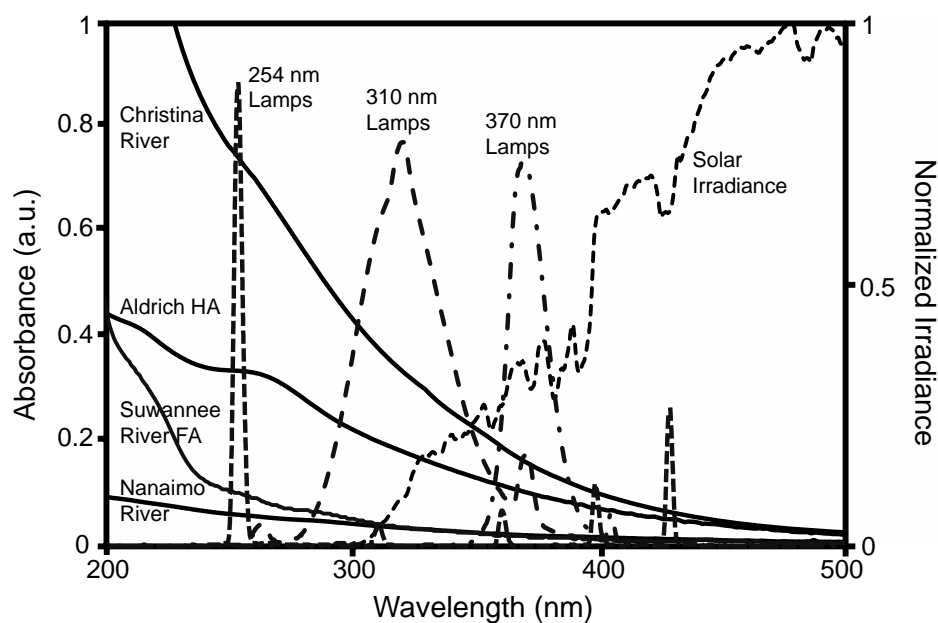


Fig. 2 UV/visible spectra of aqueous solutions and lamp profiles. Solid lines represent the absorption spectra of water samples containing DOM. Dotted lines display spectral distribution of irradiation sources. Solar irradiance is shown for comparison.

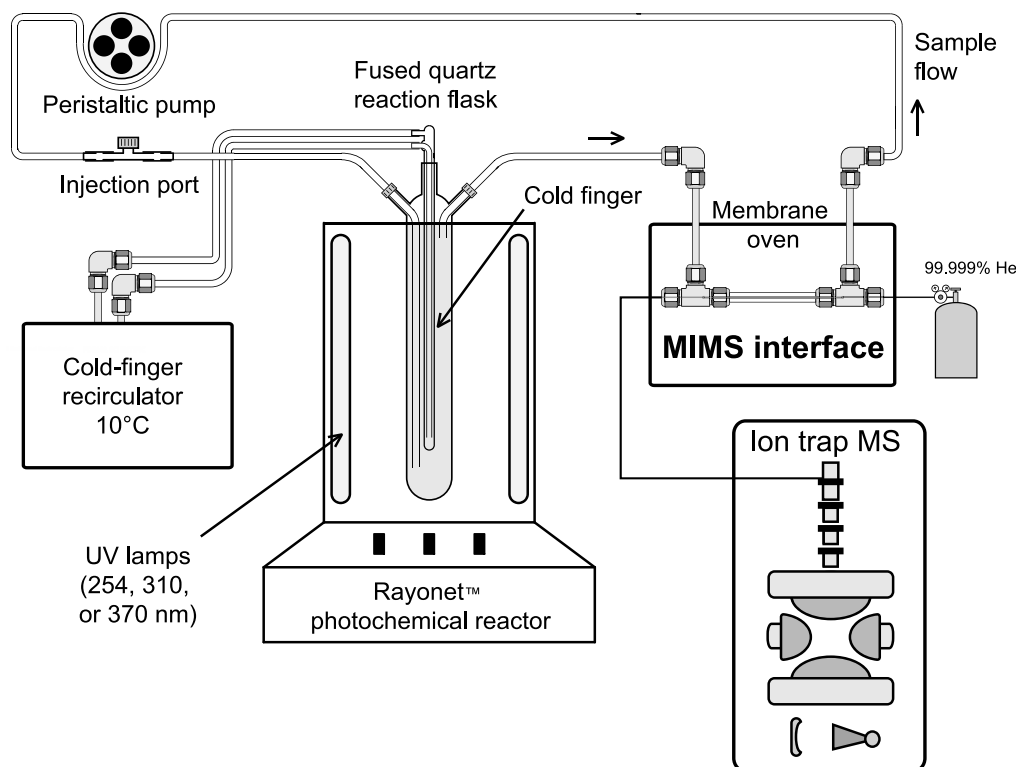


Fig. 3 Re-circulated closed loop for the photochemical degradation of S/VOCs in aqueous solution using membrane introduction mass spectrometry as an on-line reaction monitor.

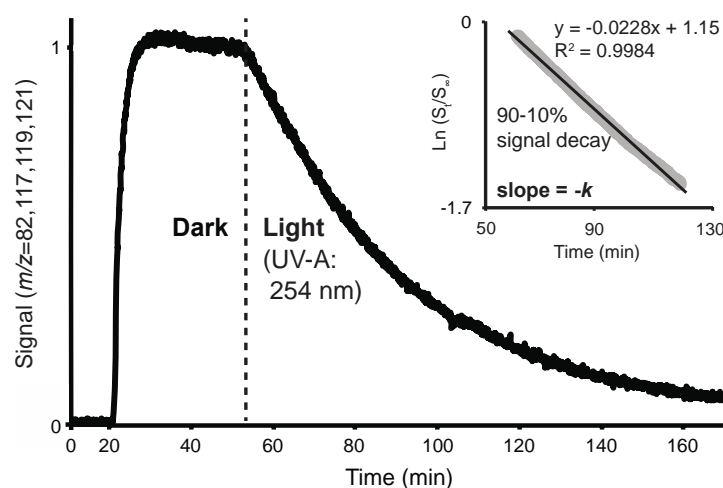


Fig. 4 Normalized signal for a 10 ppb (65 nM) solution of TCM ($m/z=82, 117, 119, 121$) illustrating photodegradation at 254 nm in de-aerated aqueous solution containing 3.3 ppm C of Aldrich humic acid (AHA). Inset shows the log transformed data showing first order kinetic behaviour and the determination of the first order rate constant, $k = 0.023 \text{ min}^{-1}$.

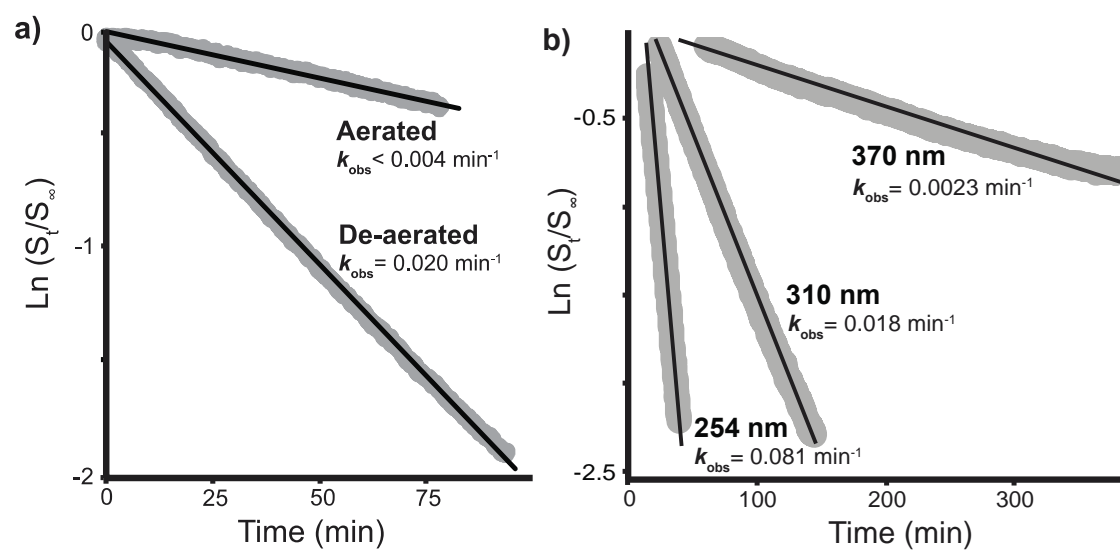


Fig. 5 Log transformed reaction profiles for the DOM photo-sensitized loss of TCM. (a) The effect of dissolved oxygen on 100 ppb TCM solutions containing AHA at 3.3 ppm C photolyzed at 254 nm. (b) The effect of wavelength on 10 ppb TCM solutions in CR water containing 18 ppm C.

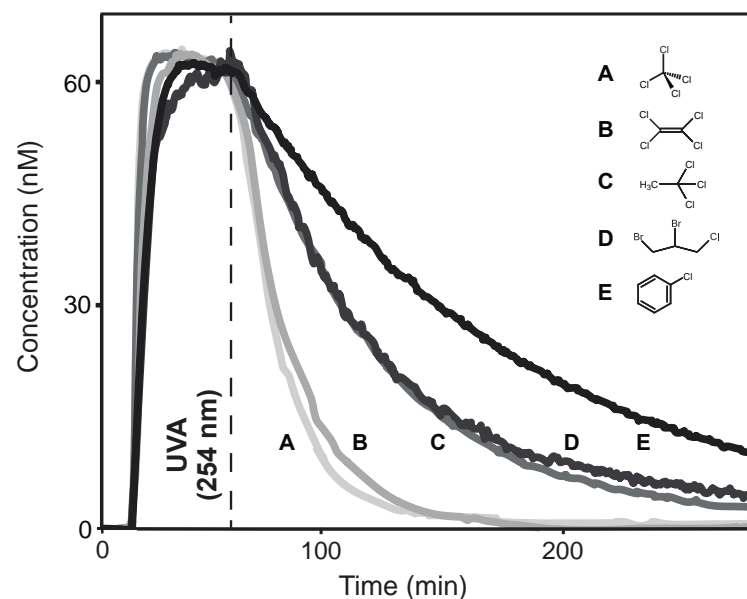


Fig. 6 Simultaneous monitoring of five halogenated contaminants at low concentration (65 nM) in de-aerated water from CR containing DOM at 18 ppm C.

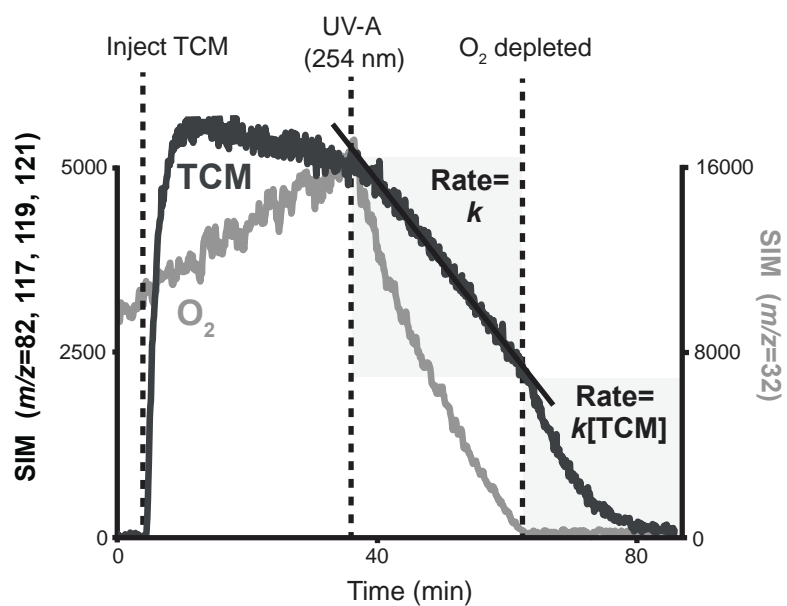
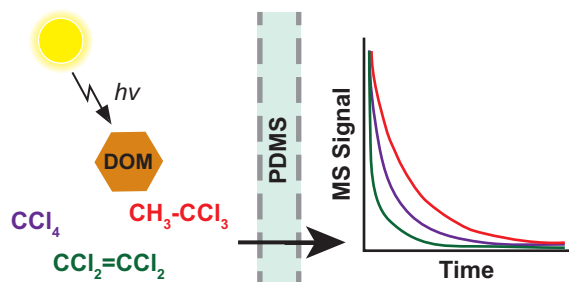


Fig. 7 Reaction of TCM in de-aerated CR water diluted to 4.4 ppm C with a SIM at m/z 32 monitoring molecular oxygen. Slow rise in O_2 after de-aeration has stopped ($t=0$ min) but before photolysis starts ($t=35$ min) represents trace oxygen (< 1 ppm). When irradiation is initiated, TCM decays with zeroth-order kinetic behaviour. After all oxygen is consumed ($t=60$ min), the TCM decay converts to first order kinetic behaviour.

Graphical Abstract and Summary Statement for Manuscript ID PP-ART-07-2015-000286 for publication in *Photochemical & Photobiological Sciences*



On-line membrane introduction mass spectrometry used to directly measure the photosensitized reductive dehalogenation kinetics of trace aqueous halocarbons in the presence of naturally occurring dissolved organic matter